Dynamic mechanical relaxation properties of poly(ether ether ketone)

R. K. Krishnaswamy and D. S. Kalika*
Department of Chemical Engineering, University of Kentucky, Lexington, KY 40506-0046, USA
(Received 4 August 1993; revised 3 September 1993)

The influence of crystalline morphology on the dynamic mechanical relaxation properties of poly(ether ether ketone) (PEEK) has been investigated for the glass–rubber (α) and sub-glass (β) relaxations; a series of both cold-crystallized and melt-crystallized specimens were examined. The presence of crystallinity had a marked influence on the glass–rubber relaxation characteristics of PEEK owing to the relative constraint imposed on the amorphous-phase motions by the crystallites. Above T_g, a progressive relaxation of rigid amorphous-phase material was evident, as well as a small incremental decrease in modulus reflecting the onset of the low-temperature melting component. The sub-glass mechanical relaxation was bimodal, comprising a lower-temperature (β_1) component, which originated in the bulk of the amorphous material, and a higher-temperature (β_2) component, which originated in organized regions of the amorphous phase (i.e. at the crystal–amorphous interphase). Both the dynamic mechanical and corresponding dielectric results displayed morphological sensitivity in the β relaxation region, with the mechanical results encompassing motions of a more complex (i.e. cooperative) nature.

(Keywords: poly(ether ether ketone); dynamic mechanical relaxation; semicrystalline morphology)

INTRODUCTION

Poly(ether ether ketone) (PEEK) is a semicrystalline engineering thermoplastic based on a relatively rigid, *para*-connected aromatic backbone structure, and displays outstanding mechanical properties in combination with exceptional thermal and chemical resistance characteristics. In analogy to other polymers of 'low crystallinity', e.g. poly(ethylene terephthalate) (PET)[1], PEEK can be quenched from the melt to a wholly amorphous glass, and thus affords an opportunity to investigate a wide range of crystalline morphologies as established over both cold-crystallization and melt-crystallization histories. The development of crystal structure and morphology in PEEK has been recently reviewed[2]. The dynamic properties of PEEK are highly sensitive to the semicrystalline morphology that develops in the material as governed by its thermal, mechanical and chemical exposure history. Both dynamic mechanical[3–11] and dielectric[3,5–7,12,13] measurements reflect a marked influence of crystallinity on the relaxation characteristics of the material. In this study, the dynamic mechanical relaxation characteristics of a series of both cold-crystallized and melt-crystallized PEEK samples are investigated across the glass–rubber relaxation and sub-glass relaxation regions. This work serves to provide an expanded understanding of PEEK relaxation phenomena as influenced by material thermal history and morphology, and allows for a direct comparison between the dynamic mechanical and dielectric relaxation behaviour of comparable PEEK samples.

* To whom correspondence should be addressed

BACKGROUND

As indicated above, the dynamic mechanical and dielectric relaxation behaviour of poly(ether ether ketone) has been explored by a number of investigators. Typically, these studies report the relaxation characteristics of amorphous PEEK, and perhaps one representative semicrystalline sample[4–11]; only recently have experimental studies appeared that consider dynamic mechanical[3] and dielectric[3,12,13] properties for a full range of crystallized specimens. Nonetheless, a comprehensive picture as to the general dynamic relaxation behaviour of amorphous and semicrystalline PEEK has begun to emerge.

The sub-glass relaxation of PEEK comprises the localized γ transition, evident at very low temperatures[3,14], and the broad β relaxation, which appears at somewhat higher temperatures. Dielectric studies by Jonas and Legras[3] reveal the γ relaxation as a shoulder in the isochronal loss *versus* temperature curve, located at approximately -125°C (400 Hz); the authors suggest that the γ relaxation originates from uncorrelated wagging of polar bridges along the polymer chains. The β relaxation encompasses a wide distribution of relatively short-range molecular motions. Dynamic mechanical measurements by David and Etienne[4] indicate that the β relaxation, in fact, comprises two overlapping components (designated β_1 and β_2, respectively, with increasing temperature): the β_1 component corresponds to a simple, non-cooperative process, while the β_2 component encompasses a cooperative element. Comparison of dynamic mechanical loss spectra for amorphous and cold-crystallized PEEK indicates an enhancement in the relative magnitude of the β_2 response for the semicrystalline sample, most likely reflecting the origin of the

0032-3861/94/06/1157–09

β_2 process in organized regions of the amorphous phase, such as in the vicinity of the crystal–amorphous interphase. Notably, the location (i.e. central relaxation time) of the β_1 and β_2 processes appears to be insensitive to the presence of crystallinity. Dynamic mechanical results reported by Sasuga and Hagiwara[8–10] are consistent with this description: three overlapping molecular processes are identified in the β relaxation region, of which the low-temperature component correlates with the presence of water in the sample. Subsequent dielectric studies[3] indicate that this component does not correspond to a separate molecular relaxation, but reflects the influence of water as a plasticizer for the primary motions inherent to the β process, leading to a decrease in isochronal relaxation temperature and an increase in relaxation magnitude with increasing water content.

Dielectric loss measurements[3,6,12] in the range of the β relaxation do not display the bimodal character that is observed in the dynamic mechanical spectra, with only a single relaxation process evident in the resulting ε'' *versus* temperature curves. A comparison of Arrhenius plots by Starkweather and Avakian[6] based on dielectric and dynamic mechanical loss data for the β relaxation indicates that the dielectric loss maxima are offset to lower temperatures as compared to the dynamic mechanical result, with a correspondingly smaller apparent activation energy. The authors conclude that the dielectric relaxation represents a low-temperature, high-frequency component of a much broader range of motions as evident in the dynamic mechanical spectrum. In contrast to the sub-glass relaxation behaviour of other 'low-crystallinity' polymers such as PET[15,16], the dielectric β relaxation in PEEK is sensitive to the presence of crystalline morphology: isochronal relaxation temperatures are offset to higher values, and a disproportionate decrease in relaxation intensity is observed for semicrystalline samples as compared to the wholly amorphous material, thus reflecting the constraining influence of the crystallites on the amorphous-phase motions inherent to the β relaxation[12]. This result suggests that the dielectric β relaxation in PEEK encompasses segmental motions of longer range and greater cooperativity than are encountered in more flexible polymers, such as PET.

Intermediate to the sub-glass (β) relaxation and the glass–rubber (α) relaxation, dynamic mechanical data indicate the presence of a structural 'relaxation' that correlates with the presence of local disordered regions within the polymer sample (designated the β' relaxation)[4,8–10]. The β' relaxation appears as a shoulder on the low-temperature side of the isochronal glass–rubber relaxation loss peak, and is most prominent in the first heating sweep of samples that have been rapidly quenched from above T_g. The β' relaxation is typically absent from subsequent heating sweeps owing to the molecular rearrangements that occur during the initial sample heating. Annealing the polymer at temperatures below T_g prior to measurement leads to a reduction in the magnitude of the β' relaxation, while irradiation of the sample (with resulting chain scission) produces an enhancement in the β' relaxation[8–10].

The glass–rubber (α) relaxation characteristics of PEEK display a strong sensitivity to crystalline morphology as measured by both dynamic mechanical[3,5,7–11] and dielectric methods[5,7,12,13]. The α relaxation in wholly amorphous PEEK (T_g(d.s.c.) $\sim$ 146°C[17]) is accompanied by a dramatic decrease in storage modulus and a sharp, narrow peak in loss tangent ($\tan\delta$); dielectric measurements reveal a corresponding incremental increase in dielectric constant (ε'). The dynamic relaxation behaviour of amorphous PEEK is complicated by the onset of cold crystallization in the vicinity of the glass transition. Cold crystallization produces an increase in the value of the storage modulus, and an additional relaxation process appears as a broad shoulder on the high-temperature side of the loss peak. This second relaxation corresponds to the onset of amorphous-phase motions which are now constrained by the presence of crystallinity in the cold-crystallized specimen (see below). Examination of the α relaxation in specimens with a pre-existing semicrystalline morphology reveals a relaxation that is considerably broaded as compared to the wholly amorphous material, and which is shifted upwards in temperature by as much as 15°C; this upward shift reflects the constraint imposed by the crystallites on the long-range motions of the glass–rubber relaxation. For cold-crystallized samples, a modest decrease in glass transition temperature is observed with increasing cold-crystallization temperature (relaxation temperatures still significantly offset as compared to the wholly amorphous sample)[3,12,13,17]. This behaviour is the result of a progressive increase in the thickness of the amorphous interlayer with increasing crystallization temperature, thus leading to a decrease in the relative constraint imposed on the amorphous-phase segments by the crystalline phase[3].

In addition to a positive offset in relaxation temperature (increased central relaxation time), the presence of crystallinity in PEEK results in a disproportionate decrease in relaxation intensity across the glass transition relative to the weight fraction crystallinity in the sample. Upon heating across the glass transition, both calorimetric[13,17] and dielectric[12,13] measurements indicate an increase in amorphous-phase chain mobility that is significantly less than that expected based on full mobilization of the non-crystalline material. This is consistent with the presence of a finite 'rigid amorphous-phase' fraction in semicrystalline PEEK, which represents the fraction of amorphous material that remains immobile across the glass transition. Dielectric studies in the temperature range just above T_g indicate a gradual increase in relaxation intensity with increasing temperature, which is consistent with the mobilization of some portion of the rigid amorphous-phase fraction prior to the onset of crystalline melting.

EXPERIMENTAL

PEEK samples were obtained as both amorphous film (Stabar K200: 5 and 10 mil (0.127 and 0.254 mm) thickness) and pellets ('Victrex' 450G) from ICI Films and ICI Advanced Materials, respectively. Cold-crystallized samples of varying crystallinity were prepared by annealing the K200 film in a temperature-controlled Carver melt press at temperatures T_a ranging from 180 to 300°C; all samples were isothermally annealed for 90 min. The thick (10 mil) films were used for the glass transition studies, while the thin (5 mil) films were used for sub-ambient (β relaxation) investigations. Melt-crystallized specimens (thickness of approximately 0.27 mm) were obtained by compression moulding the 450G pellets from the melt at moderate pressure (melt temperatures ranging from 360 to 400°C), with subsequent cooling to the solid

state either at a constant rate ($\sim 1°C\,min^{-1}$) or in a stepwise manner. In the latter case, samples were cooled at $1°C\,min^{-1}$ to 330°C, at which temperature they were annealed isothermally for 1 h. The samples were then isothermally annealed at decreasing 10°C increments (1 h at 320°C, 310°C, etc.) to 250°C, at which point they were cooled to room temperature; this cooling progression was imposed in an effort to establish a slow cooling history within the operational constraints of the melt press. The resulting crystalline weight fraction W_c was determined based on density gradient measurements (calcium nitrate/water column); the density of the amorphous (as-received) film was determined to be $\rho_a = 1.260\,g\,cm^{-3}$, and the crystal density was taken as $\rho_c = 1.400\,g\,cm^{-3}$ (ref. 18).

Dynamic mechanical properties were measured using a Polymer Laboratories dynamic mechanical thermal analyser interfaced with a Polymer Laboratories temperature controller. All samples were fully dried under vacuum prior to measurement and were investigated in an inert atmosphere. Measurements in the glass transition range were carried out in bending mode, with single cantilever geometry. Bending modulus and $\tan\delta$ were recorded at frequencies ranging from 0.1 to 30 Hz across a temperature range of 50 to 300°C; a scanning rate of $0.8°C\,min^{-1}$ was used. Measurements in the range of the sub-glass (β) relaxation were carried out in tensile mode. Tensile modulus and $\tan\delta$ were recorded at frequencies ranging from 0.3 to 30 Hz across a temperature range of -125 to $+100$°C; a scanning rate of $1.4°C\,min^{-1}$ was used.

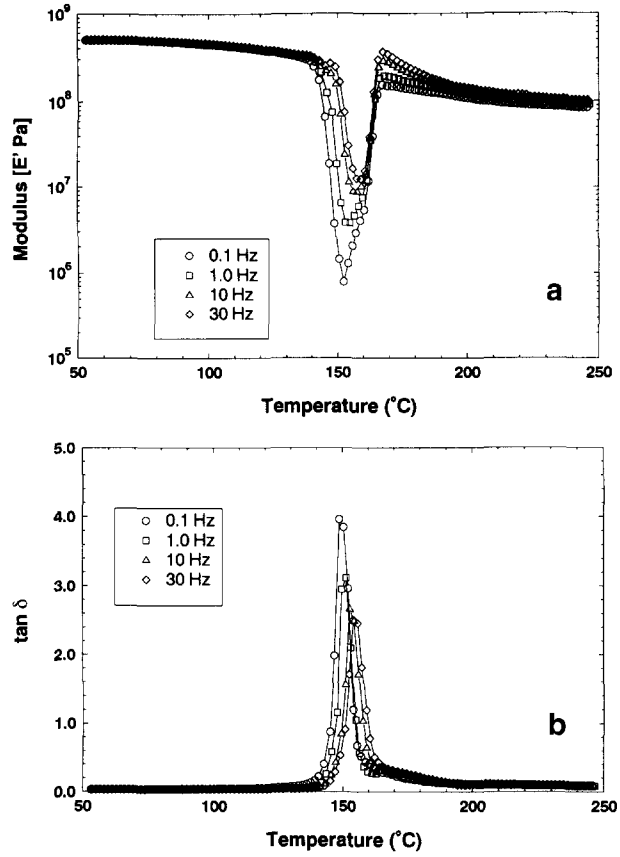

Figure 1 Dynamic mechanical results for amorphous PEEK, glass–rubber (α) relaxation. (a) Bending modulus E' (Pa) *versus* temperature (°C); (b) loss tangent ($\tan\delta$) *versus* temperature (°C): (○) 0.1 Hz, (□) 1.0 Hz, (△) 10.0 Hz, (◇) 30.0 Hz

RESULTS AND DISCUSSION

Glass–rubber (α) relaxation

Dynamic mechanical results for amorphous PEEK in the vicinity of the glass–rubber relaxation are plotted isochronally as storage modulus (E') and loss tangent ($\tan\delta$) *versus* temperature in *Figure 1*. The strong drop in storage modulus at the glass transition is followed by the onset of cold crystallization in the non-isothermal sweep, the corresponding recovery in modulus leading to a relative maximum in E' at the higher measurement frequencies. A second relaxation process is subsequently observed with increasing temperature, which corresponds to the glass–rubber relaxation of amorphous-phase chains that are now constrained by the presence of crystallinity; this second, broader relaxation is evident as a gradual decrease in modulus, and as a shoulder on the high-temperature side of the narrow peak in $\tan\delta$.

Results for a representative cold-crystallized sample ($T_a = 240$°C, $W_c = 0.29$) are shown in *Figure 2*. The presence of crystallinity leads to a considerable increase in the breadth of the relaxation as compared to the initially amorphous specimen, and a corresponding decrease in relaxation intensity. The storage modulus displays a relatively strong temperature dependence above the glass transition ($190°C < T < 240°C$), and an additional incremental decrease starting at 240°C, which reflects the 'low-temperature' melting component for this isothermally crystallized sample. Previous calorimetric studies[17] on isothermally crystallized PEEK reveal a distinct 'double-melting' behaviour, with two melting endotherms evident upon heating: a 'low-temperature' endotherm located 15 to 20°C above the isothermal annealing temperature, and a 'high-temperature' endotherm located at approximately 340°C, virtually independent of sample history. For the various cold-crystallized samples studied here, the location of this second, relatively small decrease in modulus correlates directly with isothermal annealing temperature, thus confirming its source as the 'low-temperature' melting component. Further, the magnitude of the incremental drop in modulus increases with increasing cold-crystallization temperature, in agreement with the observed trend in enthalpy for the low-temperature endotherm[17]. There has been considerable discussion as to the origin of the observed 'double melting' in PEEK, with the behaviour attributed to established morphological features in the annealed samples[19,20], or crystal melting and reorganization during heating[21]. The clear, incremental change in modulus observed here appears to be more consistent with a morphological origin as compared to a continuous melting and recrystallization process.

The weight fraction crystallinity and isochronal relaxation temperatures (T_α(1 Hz); based on maximum in $\tan\delta$) for the series of cold-crystallized samples are reported in *Table 1*. A systematic increase in crystallinity is observed with increasing annealing temperature, with the relaxation temperatures for the various semicrystalline samples offset significantly as compared to the initially amorphous specimen owing to the constraints imposed on amorphous-phase motions by the crystalline phase. A relative maximum in relaxation temperature is observed for the $T_a = 200$°C specimen, T_α decreasing for the highest cold-crystalline annealing temperatures; this result is in agreement with trends observed by both calorimetric[17] and dielectric[12,13] methods, and has been reported previously for PET[1,15,22]. Small-angle X-ray scattering

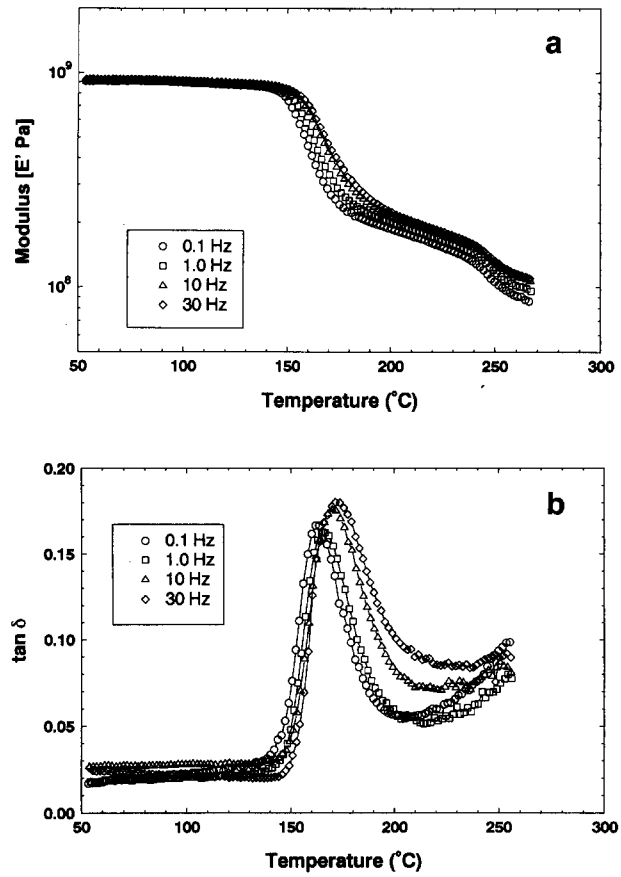

Figure 2 Dynamic mechanical results for cold-crystallized PEEK ($T_a = 240°C$, $W_c = 0.29$), glass–rubber (α) relaxation. (a) Bending modulus E' (Pa) *versus* temperature (°C); (b) loss tangent (tan δ) *versus* temperature (°C): (○) 0.1 Hz, (□) 1.0 Hz, (△) 10.0 Hz, (◇) 30.0 Hz

Table 1 Dynamic mechanical relaxation temperature for amorphous and cold-crystallized PEEK: glass–rubber (α) relaxation. T_a (°C) is isothermal cold-crystallization annealing temperature; W_c is weight fraction crystallinity based on density gradient measurements; and T_α (°C) is relaxation temperature based on maximum in tan δ (1 Hz)

Sample	T_a (°C)	W_c	T_α (°C)
A	–	0.0	152.7
1	180	0.24	167.4
2	200	0.26	167.5
3	220	0.28	167.4
4	240	0.29	166.7
5	250	0.30	166.0
6	260	0.31	165.4
7	280	0.32	164.3
8	300	0.35	163.8

(SAXS) studies by Jonas and Legras[3] clearly demonstrate an inverse relationship between glass transition temperature and the thickness of the amorphous interlayer in both cold-crystallized and melt-crystallized PEEK samples. Thus, the decrease in relaxation temperature (and corresponding decrease in central relaxation time) observed here is a manifestation of a progressive increase in crystal thickness, ultimately leading to a lessening of the constraint on the amorphous chain segments by the crystallites.

A comparison of the glass–rubber relaxation intensity for the cold-crystallized specimens is provided in terms of modulus and loss tangent in *Figures 3* and *4*, respectively. In *Figure 3*, reduced modulus ($\log E'/\log E'_0$) is plotted against reduced temperature (T/T_α) for the purpose of direct comparison of representative cold-crystallized samples. The incremental drop in modulus across the glass transition displays a systematic decrease with increasing cold-crystallization annealing temperature owing to the increase in crystalline fraction. The modulus shows a strong temperature dependence above T_g, with the observed decrease in modulus over this range being most pronounced for samples crystallized at lower temperatures: this gradual decrease in modulus is the result of the relaxation of rigid amorphous material occurring between T_g and the crystalline melting temperature. Calorimetric studies on cold-crystallized[13,17] and melt-crystallized[17] PEEK samples indicate a sizeable rigid amorphous-phase fraction at the glass transition, the quantity of which depends on the conditions of crystallization: more restrictive crystallization conditions (i.e. lower isothermal crystallization temperatures, or faster cooling rates for non-isothermal crystallization) lead to a higher rigid amorphous-phase fraction. Dielectric studies[12,13] show a progressive mobilization of some portion of the rigid amorphous material above the glass transition; the effect is strongest for samples prepared at lower cold-crystallization temperatures[12]. The dynamic mechanical data reported here are consistent with these observations, with the temperature dependence of the

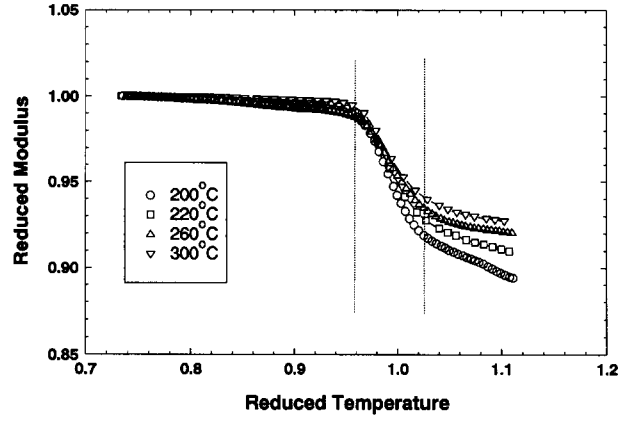

Figure 3 Reduced modulus ($\log E'/\log E'_0$) *versus* reduced temperature (T/T_α) for selected cold-crystallized PEEK samples, glass–rubber (α) relaxation: (○) $T_a = 200°C$, (□) $T_a = 220°C$, (△) $T_a = 260°C$, (▽) $T_a = 300°C$

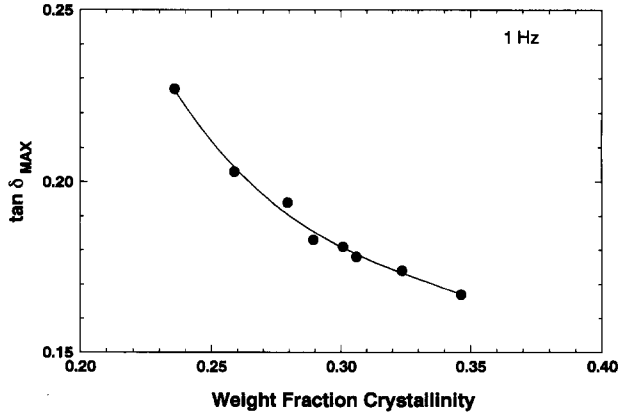

Figure 4 Magnitude of tan δ at maximum (T_α(1 Hz)) *versus* weight fraction crystallinity for cold-crystallized samples, glass–rubber (α) relaxation

modulus in this range (i.e. the slope of the log(modulus) *versus* temperature curve) greatest for those samples prepared under conditions favourable to the development of a large fraction of rigid amorphous material.

Attempts to quantify the strength of the mechanical relaxation for the various cold-crystallized samples via an empirical curve-fitting approach[1,23] were unsatisfactory owing to the difficulty in separating the primary glass–rubber relaxation from the overlapping relaxation of rigid amorphous-phase material. As noted above, however, plotting the data in a normalized manner does provide a clear qualitative indication of the reduction in relaxation strength with increasing sample crystallinity. A plot of the maximum value of tan δ *versus* bulk crystallinity (*Figure 4*, see discussion in Boyd[1]) similarly shows a systematic decrease in the intensity of the relaxation with crystallinity, consistent with an amorphous-phase origin.

The time–temperature characteristics of the mechanical glass–rubber (α) relaxation are plotted in an Arrhenius manner for amorphous and cold-crystallized PEEK in *Figure 5*; these data are based on the isochronal maxima in tan δ for the various samples. The results demonstrate the relative offset in the glass–rubber relaxation temperature for the cold-crystallized specimens relative to the initially amorphous material, with the location of the crystallized sample data shifted to the left along the reciprocal temperature axis. Data from each of the individual samples can be satisfactorily described using a WLF (Williams–Landel–Ferry) type of expression across the frequency range of investigation. The apparent activation energy for the amorphous sample (E_A) varies from 1900 kJ mol^{-1} (0.1 Hz) to 1250 kJ mol^{-1} (30 Hz). The apparent activation energies for the cold-crystallized samples are lower as compared to the amorphous specimen, with the relative activation energy increasing somewhat with increasing annealing temperature (increasing crystalline fraction). The apparent activation energy for a sample cold crystallized at 200°C, for example, ranges from 1070 kJ mol^{-1} (0.1 Hz) to 810 kJ mol^{-1} (30 Hz).

A comparison of the time–temperature results based on dynamic mechanical and dielectric[12] measurements for the amorphous and a representative cold-crystallized sample (T_a = 200°C) are provided in *Figure 6*. For

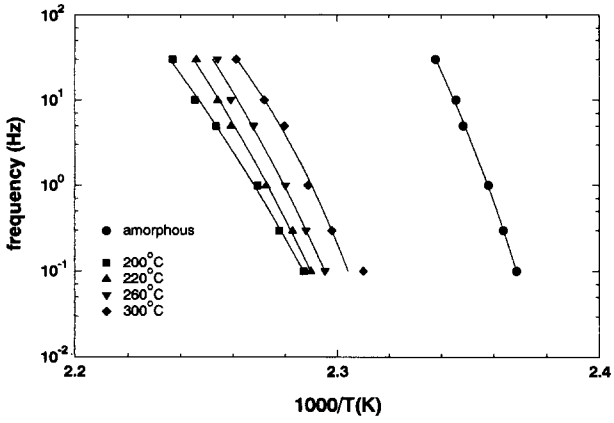

Figure 5 Arrhenius plot of frequency (Hz) *versus* $10^3/T$ (K^{-1}) based on isochronal temperature sweeps: amorphous and cold-crystallized PEEK, glass–rubber (α) relaxation: (●) amorphous, (■) T_a = 200°C, (▲) T_a = 220°C, (▼) T_a = 260°C, (◆) T_a = 300°C. Full curves represent WLF fits

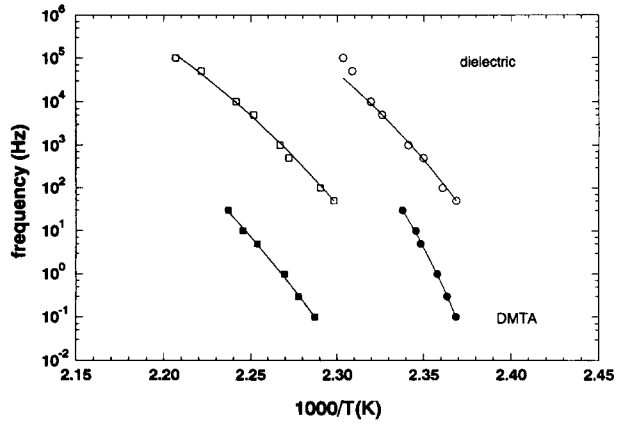

Figure 6 Arrhenius plot of frequency (Hz) *versus* $10^3/T$ (K^{-1}) based on dynamic mechanical and dielectric[12] results, glass–rubber (α) relaxation. Dynamic mechanical: (●) amorphous, (■) T_a = 200°C. Dielectric: (○) amorphous, (□) T_a = 200°C

both the amorphous and cold-crystallized samples, the dynamic mechanical relaxation temperatures (based on tan δ) are offset to higher values as compared to the dielectric result. Also, in the case of the amorphous sample, the dynamic mechanical data display a higher apparent activation energy; mechanical and dielectric data for the cold-crystallized samples indicate comparable activation energies. The behaviour observed here for the glass–rubber (α) relaxation is not unlike that reported by Starkweather and Avakian[6] for the sub-glass (β) relaxation in PEEK, in terms of both the offset in temperature for the mechanical case and the relative magnitude of the activation energy. For the β relaxation, it was demonstrated that the dielectric probe is sensitive to a relatively narrow, low-temperature component of the broad distribution of motions detectable by dynamic mechanical methods. For the longer-range motions of the α relaxation investigated here, a similar distinction in the sensitivity of the dynamic mechanical and dielectric probes is not unreasonable. It should be noted that when the α relaxation temperatures for the mechanical and dielectric data are based on the isochronal maxima in loss (E'' or ε'') as opposed to loss tangent (tan δ), the relative offset between the dynamic mechanical and dielectric results is maintained, although the magnitude of the difference is diminished.

In addition to the series of cold-crystallized samples described above, the dynamic mechanical relaxation characteristics of a group of melt-crystallized samples were investigated across the glass–rubber relaxation. Two sets of samples were considered: samples cooled continuously from the melt (1°C min^{-1}) and samples slow cooled in stepwise increments. In order to assess the possible influence of prior melt temperature on the crystallization and relaxation characteristics of the PEEK samples, melt temperatures ranging from 360 to 400°C were imposed (time at T_m ca. 10 min). Previous calorimetric studies[24,25] indicate that heating PEEK in the vicinity of its thermodynamic melting temperature (T_m° = 395°C[18]) leads to a decrease in subsequent crystallization rate and ultimate bulk crystallinity; this behaviour is attributed to the removal of self-nucleation remnants and the influence of polymer degradation. The bulk levels of crystallinity established in the various melt-crystallized samples, as well as their relaxation characteristics, are reported in *Table 2*. For the crystallization histories

Table 2 Dynamic mechanical relaxation characteristics for melt-crystallized PEEK: glass–rubber (α) relaxation. T_m(°C) is melt temperature; W_c is weight fraction crystallinity based on density gradient measurements; T_α(°C) is relaxation temperature based on maximum in $\tan\delta$ (1 Hz); and $\Delta \log E$ is incremental change in log(storage modulus/Pa), evaluated at T_α(1 Hz)

(a) Samples cooled continuously from the melt at 1°C min^{-1}

T_m(°C)	W_c	T_α(°C)	$\Delta \log E$
360	0.37	161.7	0.49
380	0.37	161.8	0.54
400	0.37	162.7	0.62

(b) Samples cooled stepwise from the melt in 10°C increments

T_m(°C)	W_c	T_α(°C)	$\Delta \log E$
360	0.40	161.5	0.48
380	0.40	162.1	0.52
400	0.39	162.8	0.54

considered here, prior melt temperature has no influence on the bulk level of crystallinity achieved: somewhat higher levels of crystallinity are observed for the incrementally cooled samples as compared to the continuously cooled specimens.

The isochronal modulus *versus* temperature curves recorded for the various melt-crystallized samples were largely consistent with those reported for the cold-crystallized samples, above. In the range between T_g and the onset of crystalline melting, however, the melt-crystallized specimens display only a weak modulus–temperature dependence, indicating minimal rigid amorphous-phase relaxation. As such, it is possible to establish a reasonable estimate of the magnitude of the relaxation strength across the glass–rubber relaxation. Specifically, the logarithms of both the unrelaxed (E_U) and relaxed (E_R) moduli were described as linear functions of temperature in ranges well below and well above the glass transition, respectively[23]:

$$\log E_U = \log E_U^0 + A(T - T_0) \qquad (T \ll T_\alpha) \qquad (1a)$$

$$\log E_R = \log E_R^0 + B(T - T_0) \qquad (T \gg T_\alpha) \qquad (1b)$$

The relaxation strength ($\Delta \log E$) was then estimated as the difference between $\log E_U$ and $\log E_R$ evaluated at the isochronal peak temperature, T_α(1 Hz). (It is acknowledged that the limiting values E_U and E_R could also be estimated based on Argand plots of E'' *versus* E' at fixed temperature; this estimation would be complicated, however, by the potential contribution of background loss to the E'' values.) Examination of the value of $\Delta \log E$ for the various melt temperatures (both cooling histories) indicates an increase in relaxation strength with increasing melt temperature, the crystalline fraction remaining constant. The enhanced degree of amorphous chain mobility (higher values of $\Delta \log E$) in those samples exposed to the highest melt temperatures is most likely a reflection of the removal of prior crystalline morphology in the as-received PEEK pellets, since a full and complete erasure of the vestigial crystalline constraints would be anticipated only for those samples prepared at melt temperatures above the thermodynamic melting temperature ($T_m = 400$°C samples). A similar result was observed for melt-crystallized specimens investigated using dielectric methods: a marked increase in dielectric relaxation intensity was indicated for samples held in the melt at temperatures above T_m° prior to crystallization[12].

Storage modulus data for a melt-crystallized sample ($T_m = 400$°C, continuous cooling) are plotted isothermally as $\log E'$ *versus* log(frequency) in *Figure 7*: the reported temperature range is 147 to 195°C. Time–temperature superposition was used to establish a master curve in modulus, with shift factor (a_T) determined based on the horizontal offset necessary to superimpose the various modulus data relative to the reference temperature of 147°C. *Figure 8* shows the resulting master curve, accompanied by a plot of shift factor (a_T) *versus* temperature (see inset). In the region of the glass transition, the dependence of shift factor on temperature can be described by the WLF equation[26]:

$$\log a_T = \frac{-C_1(T - T_0)}{C_2 + (T - T_0)} \qquad (2)$$

The best-fit values of C_1 and C_2 (determined by a linear plot of $(T - T_0)/\log a_T$ *versus* $(T - T_0)$) are $C_1 = 25.4$ and $C_2 = 90.2$ ($T_0 = 147$°C, see full curve in inset of *Figure 8*).

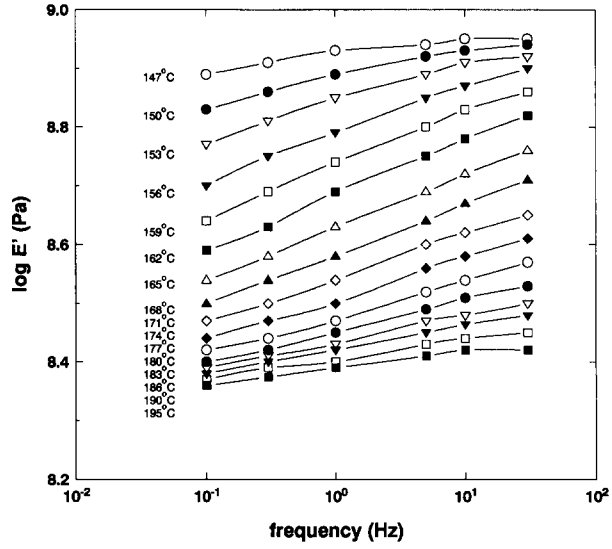

Figure 7 Bending modulus E' (Pa) *versus* frequency (Hz) at selected temperatures for melt-crystallized PEEK ($T_m = 400$°C), glass–rubber (α) relaxation

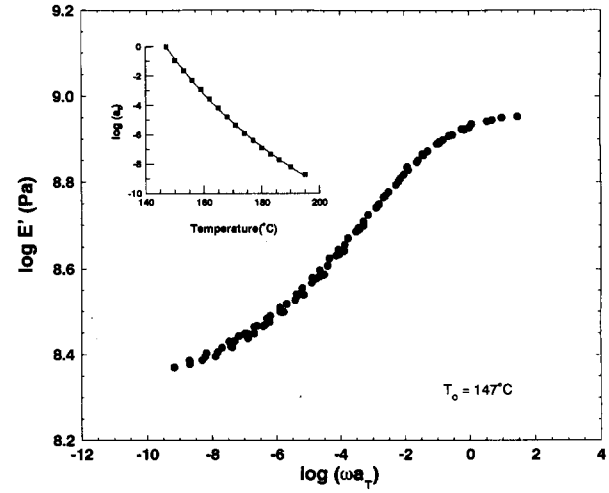

Figure 8 Modulus–frequency master curve based on time–temperature superposition; $T_0 = 147$°C. Inset: log(shift factor) *versus* temperature (°C); full curve represents WLF fit

Sub-glass (β) relaxation

Dynamic mechanical results for amorphous and cold-crystallized PEEK in the β relaxation region are presented in *Figure 9* as $\tan\delta$ *versus* temperature. The data display the same bimodal behaviour described by David and Etienne[4], and their nomenclature will be adopted here. The loss tangent result for the amorphous sample is dominated by the lower-temperature (β_1) component: the only evidence for an additional relaxation element in this case is an observed broadening on the high-temperature side of the loss peak. The sample cold crystallized at 200°C clearly displays an overlapped response of both the β_1 and β_2 components: the strength of the β_1 component is diminished in the crystallized sample as compared to the amorphous case, while the strength of the higher-temperature (β_2) component is significantly enhanced. Examination of a sample cold crystallized at 300°C indicates β_1 and β_2 components of comparable magnitude, with $\tan\delta$ now appearing as a broad, nearly symmetric peak in temperature centred approximately midway between the individual β_1 and β_2 relaxations.

The above results are consistent with the morphological assignments proposed by David and Etienne[4] and also Sasuga and Hagiwara[8–10], namely that the β_1 component originates from highly localized, non-cooperative motions in the bulk of the amorphous material, and that the β_2 component reflects more cooperative motions occurring in organized regions of the amorphous phase. In the case of the cold-crystallized samples examined here, such organized regions may exist between the crystalline and amorphous phases (i.e. in the crystal–amorphous interphase). For the sample cold crystallized at 200°C, a large fraction of rigid amorphous material is anticipated owing to the relatively restrictive crystallization conditions. The determination of rigid amorphous-phase fraction, as discussed above, provides an indication as to the degree of constraint imposed by the crystalline phase on the long-range motions of amorphous chain segments at the glass transition. Although the motions inherent to the β relaxation encompass a considerably smaller length scale, the trends observed for the relative quantity of rigid amorphous material as a function of crystallization history still provide useful insight. Specifically, comparison of the β_2 relaxation for the samples cold crystallized at 200 and 300°C shows a decrease in the relative prominence of the β_2 component for the $T_a = 300$°C sample. This behaviour is consistent with an overall decrease in rigid amorphous interphase material for samples cold crystallized at higher temperatures (i.e. less restrictive conditions), ultimately leading to a reduction in the relative β_2 response.

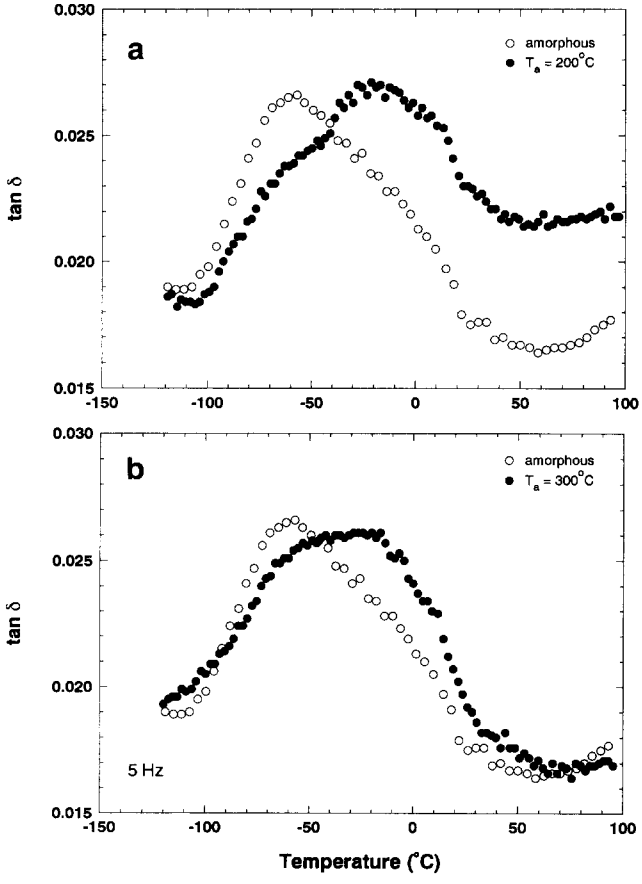

Figure 9 Dynamic mechanical loss tangent ($\tan\delta$) *versus* temperature (°C) at 5 Hz, sub-glass (β) relaxation. Amorphous and cold-crystallized PEEK: (a) (○) amorphous, (●) $T_a = 200$°C; (b) (○) amorphous, (●) $T_a = 300$°C

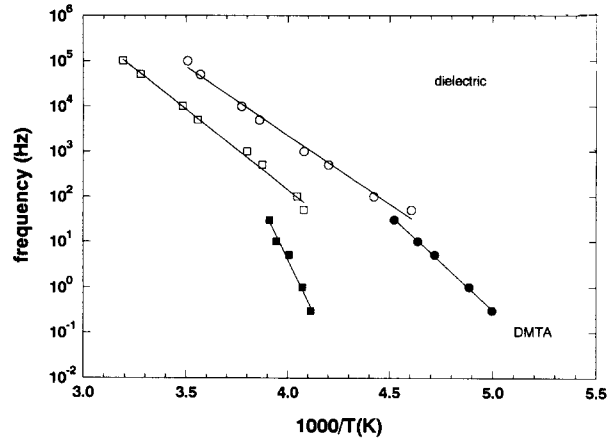

Figure 10 Arrhenius plot of frequency (Hz) *versus* $10^3/T$ (K^{-1}) based on dynamic mechanical and dielectric[12] results, sub-glass (β) relaxation. Dynamic mechanical: (●) amorphous, (■) $T_a = 200$°C. Dielectric: (○) amorphous, (□) $T_a = 200$°C

A frequency–temperature Arrhenius plot for the β relaxation region is provided in *Figure 10*; both dynamic mechanical and dielectric[12] results are reported for the amorphous material and a sample cold crystallized at 200°C. The dynamic mechanical data for the amorphous sample represent isochronal loss tangent maxima in the β_1 component, while the data for the cold-crystallized sample represent loss tangent maxima in the β_2 component. The dynamic mechanical and dielectric data reported here for the amorphous sample are largely in agreement with the results of Starkweather[6]. The apparent activation energy as determined by the slope of the log(frequency) *versus* reciprocal temperature line is $E_A = 80\,\text{kJ mol}^{-1}$ for the dynamic mechanical data and $E_A = 58\,\text{kJ mol}^{-1}$ for the dielectric result. The loss maxima for both the dynamic mechanical and dielectric measurements are shifted to higher temperatures (lower $1/T$) for the cold-crystallized ($T_a = 200$°C) specimen; in the case of the mechanical data, this reflects a shift in relaxation basis from the β_1 component to the β_2 component, but no such structure was observed in the dielectric studies. Apparent activation energies for the semicrystalline sample are $177\,\text{kJ mol}^{-1}$ (dynamic mechanical, β_2) and $68\,\text{kJ mol}^{-1}$ (dielectric), respectively.

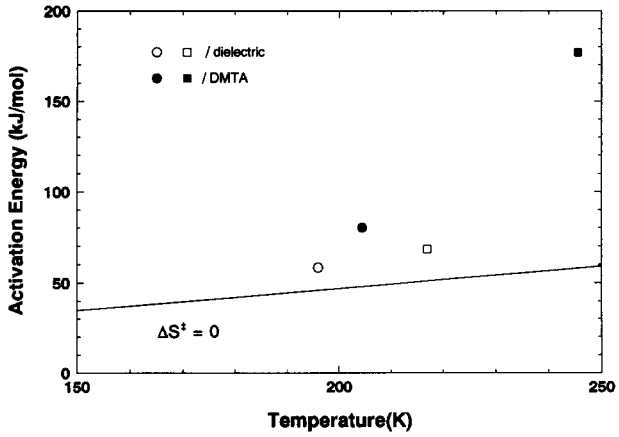

Figure 11 Apparent activation energy (kJ mol^{-1}) *versus* relaxation temperature (K) based on dynamic mechanical and dielectric[12] results, sub-glass (β) relaxation. Same symbols as *Figure 10*. Full line represents $\Delta S = 0$

Additional insight as to the nature of the detected sub-glass relaxations is afforded by consideration of the activation entropy $\Delta S^{\ddagger}$ for the different specimens and measurement techniques. Starkweather[6,27] has shown that the apparent activation energy E_A can be related to the relaxation temperature T' and the activation entropy at a frequency of 1 Hz by:

$$E_A = RT'[1 + \ln(kT'/2\pi h)] + T'\Delta S^{\ddagger} \quad (3)$$

For simple, non-cooperative relaxations with zero activation entropy, this reduces to:

$$E_A = RT'[1 + \ln(kT'/2\pi h)] \quad (4)$$

Figure 11 shows a plot of apparent activation energy *versus* relaxation temperature (1 Hz) for both the dynamic mechanical and dielectric results in the region of the β relaxation (amorphous and $T_a = 200°C$ sample); the limiting case of zero activation entropy ($\Delta S^{\ddagger} = 0$, from equation (4)) is represented by a full line. The dielectric result for the amorphous sample approaches the zero-entropy limit, the vertical distance between the data point and the full line reflecting the value of $T'\Delta S^{\ddagger}$; this indicates the sensitivity of dielectric measurement to simple, localized motions in the wholly amorphous material. The dielectric result for the cold-crystallized sample shows a somewhat greater positive offset from the zero-entropy limit, which may reflect an increased degree of cooperation required to overcome the constraints imposed on the sub-glass dipolar motions by the crystalline phase. In the case of the dynamic mechanical results, markedly higher activation entropies are observed for both the amorphous (β_1 component) and semicrystalline (β_2 component) specimens, reflecting the sensitivity of the mechanical probe to a wider spectrum of coperative motions[6]. The deviation from the zero-entropy limit is particularly significant for the β_2 relaxation, which is consistent with its probable origin at the crystal–amorphous interphase.

CONCLUSIONS

A comprehensive investigation of the dynamic mechanical relaxation characteristics of poly(ether ether ketone) in the glass–rubber (α) and sub-glass (β) relaxation regions has been completed, with an emphasis on the influence of semicrystalline morphology on relaxation properties. The presence of crystallinity had a marked impact on the α relaxation characteristics of the various cold-crystallized specimens as compared to the wholly amorphous material, the constraining influence of the crystallites producing considerable relaxation broadening and a positive offset in relaxation temperature. The magnitude of the temperature offset was reduced somewhat for the highest cold-crystallization annealing temperatures owing to an apparent increase in amorphous interlayer thickness. A strong modulus–temperature dependence was observed in the region above T_g, which reflected the progressive mobilization of some portion of the rigid amorphous-phase fraction; this feature was diminished for samples cold crystallized at higher temperatures, and for specimens crystallized from the melt. Also, a second incremental decrease in modulus was evident at higher temperatures (i.e. in the vicinity of the isothermal annealing temperature) corresponding to the low-temperature crystalline melting component. The relaxation characteristics of specimens crystallized via cooling from the melt displayed a sensitivity to prior melt temperature consistent with full removal of the initial, as-received material morphology only at temperatures above T_m°. The relative absence of an overlapping rigid amorphous-phase relaxation in the melt-crystallized samples accommodated the application of time–temperature superposition for the development of a modulus–frequency master curve: the resulting shift factor–temperature behaviour followed the WLF relation.

Dynamic mechanical measurements in the β relaxation region indicated a bimodal behaviour, with the lower-temperature β_1 component dominating in the wholly amorphous material, and the higher-temperature β_2 component most prominent in the crystallized samples. The relative strength of the β_2 component was greatest for those samples cold crystallized at lower temperatures, consistent with a relaxation origin at the crystal–amorphous interphase. Examination of the activation entropy ($\Delta S^{\ddagger}$) for the dynamic mechanical relaxation elements indicated a considerable complex (i.e. cooperative) character as compared to the observed sub-glass dielectric relaxation.

REFERENCES

1 Boyd, R. H. *Polymer* 1985, **26**, 323
2 Medellin-Rodriguez, F. J. and Phillips, P. J. *Polym. Eng. Sci.* 1990, **30**, 860
3 Jonas, A. and Legras, R. *Macromolecules* 1993, **26**, 813
4 David, L. and Etienne, S. *Macromolecules* 1992, **25**, 4302
5 D'Amore, A., Kenny, J. M., Nicolais, L. and Tucci, V. *Polym. Eng. Sci.* 1990, **30**, 314
6 Starkweather, H. W. and Avakian, P. *Macromolecules* 1989, **22**, 4060
7 Goodwin, A. A. and Hay, J. N. *Polym. Commun.* 1989, **30**, 288
8 Sasuga, T. and Hagiwara, M. *Polymer* 1985, **26**, 501
9 Sasuga, T. and Hagiwara, M. *Polymer* 1986, **27**, 821
10 Sasuga, T. and Hagiwara, M. *Polymer* 1987, **28**, 1915
11 Stober, E. J., Seferis, J. C. and Keenan, J. D. *Polym. Eng. Sci.* 1984, **25**, 1845
12 Kalika, D. S. and Krishnaswamy, R. K. *Macromolecules* 1993, **26**, 4252
13 Huo, P. and Cebe, P. *Macromolecules* 1992, **25**, 902
14 Ahlborn, K. *Cryogenics* 1988, **28**, 234
15 Coburn, J. C. and Boyd, R. H. *Macromolecules* 1986, **19**, 2238
16 McCrum, N. G., Read, B. E. and Williams, G. 'Anelastic and Dielectric Effects in Polymeric Solids', Wiley, New York, 1967
17 Cheng, S. Z. D., Cao, M. Y. and Wunderlich, B. *Macromolecules* 1986, **19**, 1868
18 Blundell, D. J. and Osborn, B. N. *Polymer* 1983, **24**, 953

19 Bassett, D. C., Olley, R. H. and Al Raheil, I. A. M. *Polymer* 1988, **29**, 1745
20 Marand, H. and Prasad, A. *Macromolecules* 1992, **25**, 1731
21 Lee, Y., Porter, R. S. and Lin, J. S. *Macromolecules* 1989, **22**, 1756
22 Illers, K. H. and Breuer, H. *J. Colloid Sci.* 1963, **18**, 1
23 Boyd, R. H. *Macromolecules* 1984, **17**, 903
24 Lee, Y. and Porter, R. S. *Macromolecules* 1988, **21**, 2770
25 Jonas, A. and Legras, R. *Polymer* 1991, **32**, 2691
26 Ferry, J. D. 'Viscoelastic Properties of Polymers', Wiley, New York, 1980
27 Starkweather, H. W. *Macromolecules* 1981, **14**, 1277